JACS
JOURNAL OF THE AMERICAN CHEMICAL SOCIETY

COMMUNICATION

pubs.acs.org/JACS

Immobilization of MP-11 into a Mesoporous Metal−Organic Framework, MP-11@mesoMOF: A New Platform for Enzymatic Catalysis

Vasiliki Lykourinou,[§] Yao Chen,[§] Xi-Sen Wang, Le Meng, Tran Hoang, Li-June Ming,* Ronald L. Musselman, and Shengqian Ma*

Department of Chemistry, University of South Florida, 4202 East Fowler Avenue, Tampa, Florida 33620, United States

Supporting Information

ABSTRACT: Microperoxidase-11 has for the first time been successfully immobilized into a mesoporous metal−organic framework (MOF) consisting of nanoscopic cages and it demonstrates superior enzymatic catalysis performances compared to its mesoporous silica counterpart.

Enzymes are nature's catalysts, featuring high reactivity, selectivity, and specificity under mild conditions.[1] Enzymatic catalysis has long been of great interest to chemical, pharmaceutical, and food industries.[2] However, the use of enzymes for industrial applications is often handicapped by their low operational stability, difficult recovery, and lack of reusability under operational conditions.[3] Immobilization of enzymes on solid supports can enhance enzyme stability as well as facilitate separation and recovery for reuse while maintaining activity and selectivity.[4] In this content, extensive attention has been paid to immobilizing enzymes into mesoporous silica materials that offer high surface areas with tunable, uniform pores.[3,4] Nevertheless, due to the lack of specific interactions with enzyme molecules, mesoporous silica materials suffer from leaching of the immobilized enzyme during the reaction process, which in return results in loss of activity upon reuse.[3,4] Although postsynthetic modification of pore walls with functional organic groups, which can provide specific interactions with the immobilized enzymes, has been widely pursued as a strategy to prevent leaching, this inevitably leads to signifcant decrease of enzyme loading and/or blockage of the channels.[4] Several attributes have been delineated for an ideal host matrix: (i) a hierarchy of pore sizes including large pores for enzyme ingress and small pores to allow diffusion of reactants and products, (ii) high surface area to ensure a high enzyme loading, (iii) large cages decorated with functional organic groups that interact with enzyme molecules and prevent leaching, and (iv) sustained framework integrity under typical reaction conditions.[4]

Over the past decade, a new type of porous materials, porous metal−organic frameworks (MOFs), has emerged.[5] Their amenability to be designed with specific functionality together with their extra-large surface areas not only makes them stand out of traditional porous materials,[6] but also promises great potential for applications such as gas storage/separation,[7] sensor,[8] magnetism,[9] and catalysis.[10] That their nanoscale features can be decorated with functional organic groups for specific interactions with biomolecules makes them appealing to stabilize enzymes for catalytic applications.[11] Although small catalytically active guest species such as organometallic compounds[12] and metalloporphyrins[13] have been successfully encapsulated into porous MOFs, the micropore size of most MOFs precludes the entry of larger-sized enzymes and could result in only surface adsorption.[14] Nevertheless, recent advances in mesoporous MOFs[15] may provide opportunities for enzymatic catalysis although, to the best of our knowledge, the exploration of mesoporous MOFs for enzymatic catalysis applications has not yet been exploited. In this contribution, we demonstrate the successful immobilization and characterization of microperoxidase-11 (MP-11) into a mesoporous MOF, and the resulting MP-11@mesoMOF exhibits superior enzymatic catalysis performances compared to the mesoporous silica counterpart.

MP-11 has dimensions of about 3.3 × 1.7 × 1.1 nm.[16] It consists of an iron-heme group linked with an α-helical undecapeptide chain via two thioether bonds of cysteine residues and a coordinated histidine residue at an axial position of the Fe(III)-heme center (Figure 1a). It is able to oxidize a wide range of organic molecules using hydrogen peroxide.[17] The mesoporous MOF we selected for MP-11 immobilization was a recently reported porous MOF,[18] Tb-TATB (hereafter denoted Tb-mesoMOF), which contains nanoscopic cages of 3.9 and 4.7 nm in diameter (Figure 1b,c). It exhibits characteristic type-IV N_2 sorption isotherms (Figure 2a) with pore sizes dominantly distributed around 3.0 and 4.1 nm in addition to a small portion of micropore size around 0.9 nm (Figure 2b). These nanoscopic cages provide adequate space to accommodate MP-11, which should be able to enter Tb-mesoMOF through the mesopores of 3.0 and 4.1 nm.

To immobilize MP-11, freshly synthesized Tb-mesoMOF crystals were immersed in MP-11 solution of HEPES (4-(2-hydroxyethyl)-1-piperazineethanesulfonic acid) buffer, and placed in an incubator at 37 °C. The uptake of MP-11 by Tb-mesoMOF was monitored by the disappearance of the Soret band at 400 nm in the supernatant,[19] and a loading of 19.1 μmol/g was reached after ∼50 h. The MP-11 saturated Tb-mesoMOF sample (hereafter denoted MP-11@Tb-mesoMOF) was then washed with fresh buffer solution several times until the supernatant became colorless to fully remove the surface adsorbed MP-11. As displayed in Figure 2c, the color of Tb-mesoMOF crystals turns dark red after being saturated with MP-11. Single crystal optical

Received: April 25, 2011
Published: June 17, 2011

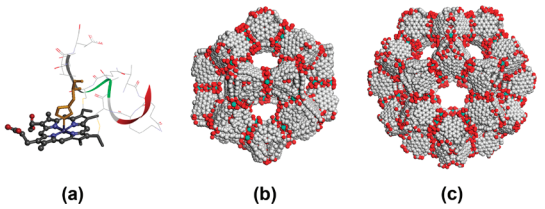

Figure 1. (a) Molecular structure of MP-11 (obtained from the solution structure of PDB 1OCD); (b) 3.9 nm-diameter cage, and (c) 4.7 nm-diameter cage in Tb-mesoMOF.

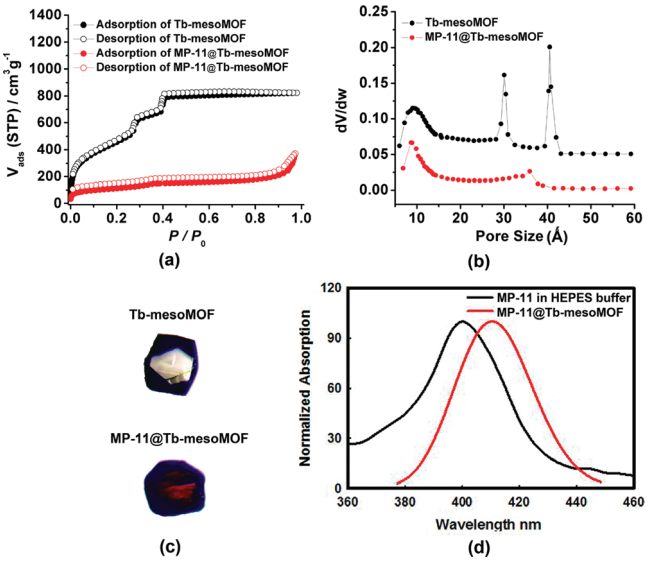

Figure 2. (a) N_2 sorption isotherms, and (b) pore size distributions of Tb-mesoMOF and MP-11@Tb-mesoMOF; (c) optical images of Tb-mesoMOF and MP-11@Tb-mesoMOF; (d) normalized single-crystal absorbance spectrum derived from specular reflectance for MP-11@Tb-mesoMOF (red) and solution optical spectrum for free MP-11 in buffer solution (black).

absorption spectroscopy studies revealed that the spectrum of MP-11@Tb-mesoMOF exhibits a Soret band at ~410 nm, while the corresponding Soret band of MP-11 in buffer solution is 400 nm (Figure 2d); the bathochromic shift of the encapsulated MP-11 in the Tb-mesoMOF is indicative of the interactions between the trapped MP-11 molecules and the hydrophobic nanoscopic cages.[20] N_2 sorption isotherms (Figure 2a) measured at 77 K indicated that the BET surface area of Tb-mesoMOF decreases from 1935 m^2/g (Langmuir surface 3247 m^2/g) to 400 m^2/g (Langmuir surface 615 m^2/g) after saturation with MP-11, indicating a majority of the free space in Tb-mesoMOF is occupied by MP-11 molecules. Pore size distribution analysis revealed that the pore size of MP-11@Tb-mesoMOF is predominately around 0.9 nm, while the pores of 4.1 and 3.0 nm observed in Tb-mesoMOF disappeared (Figure 2b). We inferred from these observations that MP-11 molecules should reside in the nanoscopic cages after saturation, while the remaining micropores of 0.9 nm can provide a mechanism for substrates to access the active MP-11 centers housed therein.

MP-11 is well-known to conduct peroxidation of organic molecules by the use of hydrogen peroxide.[17] Unfortunately, free MP-11 tends to aggregate in solution, which leads to less

Scheme 1. Reaction Scheme for Oxidation of 3,5-Di-*t*-butyl-catechol to *o*-Quinone

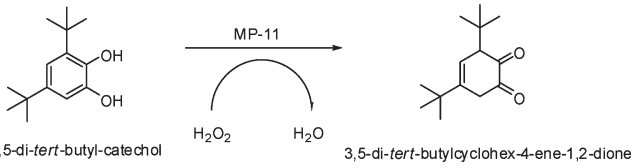

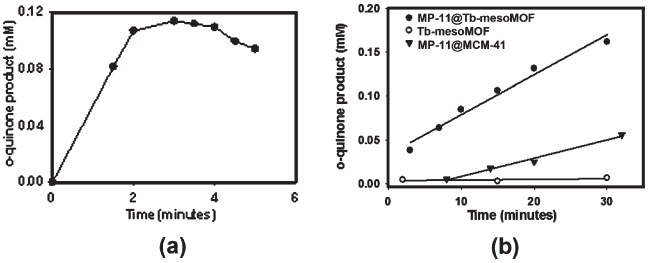

Figure 3. Kinetic traces for the oxidation of DTBC by (a) free MP-11 in HEPES buffer (0.6 μM); (b) MP-11@Tb-mesoMOF (2.0 mg), Tb-mesoMOF(2.0 mg), and MP-11@MCM-41 (2.0 mg) in methanol with H_2O_2.

accessibility for the heme, thus, adversely affecting its activity.[21] Immobilization in a suitable host material prevents aggregation, renders the heme more accessible to substrates,[22] and allows a broad range of solution conditions. Mesoporous silica materials have been widely investigated for enzyme immobilization,[3,4] and we selected MCM-41 for comparison. MCM-41 adsorbs MP-11 (hereafter denoted MP-11@MCM-41) with a lower loading capacity of 3.4 μmol/g presumably due to its lower surface area (BET surface area: ~1000 m^2/g) compared to Tb-mesoMOF. Catalytic experiments were performed for MP-11@Tb-mesoMOF, MP-11@MCM-41, free MP-11, and Tb-mesoMOF.

As polyphenols are routinely used to evaluate the peroxidase activity of porphyrin catalysts,[23] the catalytic activities of MP-11@Tb-mesoMOF and MP-11@MCM-41 were assessed by monitoring the oxidation of the chromogenic substrate 3,5-di-*t*-butyl-catechol (DTBC) at 420 nm for the formation of the corresponding *o*-quinone product (Scheme 1).[23] The reactions for MP-11@Tb-mesoMOF, MP-11@MCM-41, and Tb-mesoMOF were performed at room temperature in methanol solution with H_2O_2 added, while the catalytic activity of free MP-11 was investigated in HEPES buffer due to its insolubility and complete inactivity in methanol.

Free MP-11 in HEPES buffer solution demonstrates a fast initial rate of 8.93×10^{-4} mM/s (Figure 3a; Table 1) as derived from the slope in the first 2 min. However, it starts to lose activity after only 3 min due to the aggregation in solution.[21] Without MP-11, the reaction for Tb-mesoMOF is going very slowly with a rate of only 2.62×10^{-6} mM/s; in comparison, MP-11@MCM-41 reacts more than 10 times faster with a rate of 3.57×10^{-5} mM/s (without MP-11, MCM-41 also demonstrates a very slow reaction rate as shown in Supporting Information Figure S3). An even higher rate of 7.58×10^{-5} mM/s is observed for MP-11@Tb-mesoMOF during the initial time period of ~30 min (Figure 3b, Table 1).

After 25 h (Table 1), no more *o*-quinone was generated, and a low final conversion of 12.3% was found for free MP-11 in buffer

dx.doi.org/10.1021/ja2038003 |J. Am. Chem. Soc. 2011, 133, 10382–10385

Table 1. Summary of Catalysis Results of Oxidizing DTBC to *o*-Quinone in the Presence of 10 mM H_2O_2 in Methanol

	free MP-11[a]	Tb-mesoMOF	MP-11@MCM-41	MP-11@Tb-mesoMOF
Rate (mM/s)[b]	8.93×10^{-4} [c]	2.62×10^{-6}	3.57×10^{-5}	7.58×10^{-5}
Conversion (%)[d]	12.3	12.2	17.0	48.7

[a] Diluted to 0.6 μM in HEPES buffer. [b] Rate calculated from the first 30 min. [c] Initial rate calculated in the first 2 min. [d] Final conversion after 25 h.

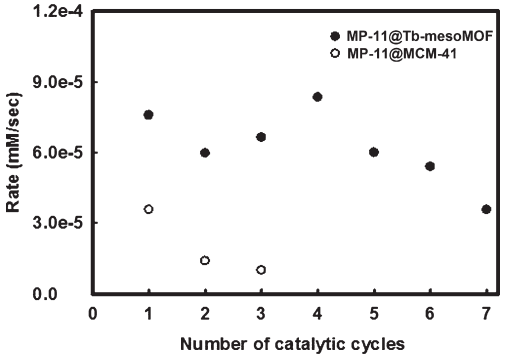

Figure 4. Reaction rates of MP-11@Tb-mesoMOF and MP-11 @MCM-41 at different cycles.

solution, which can be ascribed to the fast deactivation of MP-11 as a result of aggregation in solution. A final conversion of 12.2% was observed for Tb-mesoMOF in methanol solution, meaning Tb-mesoMOF exhibits low activity for the oxidation of DTBC to *o*-quinone. MP-11@MCM-41 demonstrated an enhanced activity with a final conversion of 17.0%, but the catalyst was bleached out owing to the leaching of MP-11 during the assay (Figure S6). In contrast, the color of MP-11@Tb-mesoMOF remained dark red with no MP-11 found in the supernatant after the reaction, and a much higher conversion of 48.7% was obtained (Table 1). These experiments indicated that the microperoxidase catalyst was greatly stabilized through the mesoporous MOF host matrix.

We evaluated the recyclability of MP-11@Tb-mesoMOF by checking its catalytic activities at different cycles. As shown in Figure 4, the reaction rate of MP-11@Tb-mesoMOF fluctuates from 5.40×10^{-5} to 8.34×10^{-5} mM/s in the first six cycles; it decreases to 3.56×10^{-5} mM/s at the seventh cycle, representing ~53% activity drop compared to that of the first cycle (Table S1). In comparison, the activity of MP-11@MCM-41 decreases abruptly with more than 60% activity lost after the first cycle, and only 28% activity remains at the third cycle (Table S1). The fast decay of MP-11@MCM-41 originates from the leaching of MP-11, which was detected in the supernatant (Figure S6). No MP-11 leaching was observed for MP-11@Tb-mesoMOF over seven cycles, and the Tb-mesoMOF host could still maintain its framework intregrity after catalytic cycles as evidenced by the powder X-ray diffraction studies (Figure S7). We reasoned that the capability of MP-11@Tb-mesoMOF to retain activity for at least six cycles could be attributed to the strong hydrophobic interactions between the Tb-mesoMOF framework and MP-11 molecules trapped in the hydrophobic nanoscopic cages, preventing their escape from the MOF host matrix.

In summary, we have demonstrated for the first time the successful immobilization of microperoxidase-11 into a mesoporous MOF consisting of nanoscopic cages, which exhibited superior enzymatic catalysis performances compared to mesoporous silica material MCM-41. The high catalytic activity together with recyclability and solvent adaptability for MP-11 encapsulated in the Tb-mesoMOF with a well-defined structure promises that mesoporous MOFs might serve as a new type of host matrix material to immobilize enzymes for catalysis applications in organic solvents. Considering the richness of mesoporous MOF structures, the present studies also open a new avenue for enzyme immobilization as heterogeneous biocatalysts. Ongoing work in our laboratory is exploring and designing new mesoporous MOFs to immobilize different kinds of enzymes for catalysis applications under various conditions.

■ ASSOCIATED CONTENT

Supporting Information. Experimental procedures for MP-11 uptake and examination of the catalytic activities, single-crystal specular reflectance spectroscopy, plots of kinetic traces, table of reaction rates, and PXRD patterns. This material is available free of charge via the Internet at http://pubs.acs.org.

■ AUTHOR INFORMATION

Corresponding Author
sqma@usf.edu; ming@usf.edu

Author Contributions
[§]These authors contributed equally.

■ ACKNOWLEDGMENT

The authors acknowledge the University of South Florida for financial support of this work. This work was also supported, in part, by the University of South Florida Internal Awards Program under Grant No.18325. Support from NSF (L.-J.M.; CHE-0718625) on metallopeptides is also acknowledged. The authors also thank Prof. Mike Zaworotko for helpful discussions, and the reviewer for constructive comments and suggestions.

■ REFERENCES

(1) Reedy, C. J.; Gibney, B. R. *Chem. Rev.* **2004**, *104*, 617–650.
(2) Schmid, A.; Dordick, J. S.; Hauer, B.; Kiener, A.; Wubbolts, M.; Wtholt, B. *Nature* **2001**, *409*, 258–268.
(3) Hartmann, M.; Jung, D. *J. Mater. Chem.* **2010**, *20*, 844–857.
(4) (a) Hartmann, M. *Chem. Mater.* **2005**, *17*, 4577–4593. (b) Hudson, S.; Cooney, J.; Magner, E. *Angew. Chem., Int. Ed.* **2008**, *47*, 8582–8594.
(5) Long, J. R.; Yaghi, O. M. *Chem. Soc. Rev.* **2009**, *38*, 1213–1214.
(6) (a) Kitagawa, S.; Kitaura, R.; Noro, S.-i. *Angew. Chem., Int. Ed.* **2004**, *43*, 2334–2375. (b) Morris, R. E.; Wheatley, P. S. *Angew. Chem., Int. Ed.* **2008**, *47*, 4966–4981. (c) Férey, G. *Chem. Soc. Rev.* **2008**, *37*, 191–214. (d) Ma, S.; Zhou, H.-C. *Chem. Commun.* **2010**, *46*, 44–53. (e) Ma, S.; Meng, L. *Pure Appl. Chem.* **2011**, *83*, 167–188.
(7) (a) Ma, S. *Pure Appl. Chem.* **2009**, *81*, 2235–2251. (b) Li, J.-R.; Kuppler, R. J.; Zhou, H.-C. *Chem. Soc. Rev.* **2009**, *38*, 1477–1504. (c) Murray, L. J.; Dinca, M.; Long, J. R. *Chem. Soc. Rev.* **2009**, *38*, 1294–1314.
(8) (a) Allendorf, M. D.; Bauer, C. A.; Bhakta, R. K.; Houk, R. J. T. *Chem. Soc. Rev.* **2009**, *38*, 1330–1352. (b) Lan, A. J.; Li, K. H.; Wu, H. H.;

Olson, D. H.; Emge, T. J.; Ki, W.; Hong, M. C.; Li, J. *Angew. Chem., Int. Ed.* **2009**, *48*, 2334–2338. (c) Chen, B.; Xiang, S.; Qian, G. *Acc. Chem. Res.* **2010**, *43*, 1115–1124.

(9) Kurmoo, M. *Chem. Soc. Rev.* **2009**, *38*, 1353–1379.

(10) (a) Lee, J.; Farha, O. K.; Roberts, J.; Scheidt, K. A.; Nguyen, S. T.; Hupp, J. T. *Chem. Soc. Rev.* **2009**, *38*, 1450–1459. (b) Ma, L. Q.; Abney, C.; Lin, W. B. *Chem. Soc. Rev.* **2009**, *38*, 1248–1256. (c) Corma, A.; Garcıa, H.; Llabreés i Xamena, F. X. *Chem. Rev.* **2010**, *110*, 4606–4655.

(11) (a) Perry, J. J.; Perman, J. A.; Zaworotko, M. J. *Chem. Soc. Rev.* **2009**, *38*, 1400–1417. (b) Tanabe, K. K.; Cohen, S. M. *Chem. Soc. Rev.* **2011**, *40*, 498–519.

(12) Hermes, S.; Schröter, M.-K.; Schmid, R.; Jhodeir, L.; Muhler, M.; Tissler, A.; Fischer, R. W.; Fischer, R. A. *Angew. Chem., Int. Ed.* **2005**, *44*, 6237–6240.

(13) (a) Alkordi, M. H.; Liu, Y. L.; Larsen, R. W.; Eubank, J. F.; Eddaoudi, M. *J. Am. Chem. Soc.* **2008**, *130*, 12639–12641. (b) Kockrick, E.; Lescouet, T.; Kudrik, E. V.; Sorokin, A. B.; Farrusseng, D. *Chem. Commun.* **2011**, *47*, 1562–1564.

(14) Pisklak, T. J.; Macias, M.; Coutinho, D. H.; Huang, R. S.; Balkus, K. J. *Top. Catal.* **2006**, *38*, 269–278.

(15) Fang, Q.-R.; Makal, T. A.; Young, M. D.; Zhou, H.-C. *Comments Inorg. Chem.* **2010**, *31*, 165–195.

(16) Marques, H. *Dalton Trans.* **2007**, *39*, 4371–4385.

(17) Veeger, C. *J. Inorg. Biochem.* **2002**, *91*, 35–45.

(18) Park, Y. K.; Choi, S. B.; Kim, H.; Kim, K.; Won, B.-H.; Choi, K.; Choi, J.-S.; Ahn, W.-S.; Won, N.; Kim, S.; Jung, D. H.; Choi, S.-H.; Kim, G.-H.; Cha, S.-S.; Jhon, Y. H.; Yang, J. K.; Kim, J. *Angew. Chem., Int. Ed.* **2007**, *46*, 8230–8233.

(19) Nakamura, S.; Mashino, T.; Hirobe, M. *Tetrahedron Lett.* **1992**, *33*, 5409–5412.

(20) Uchida, T.; Ishimori, K.; Morishima, I. *J. Biol. Chem.* **1997**, *272*, 30108–30114.

(21) Kadnikova, E. N.; Kostic, N. M. *J. Org. Chem.* **2003**, *68*, 2600–2608.

(22) Yan, A. X.; Li, X. W.; Ye, Y. H. *Appl. Biochem. Biotechnol.* **2002**, *101*, 113–129.

(23) Kawamura-Konishi, Y.; Asano, A.; Yamazaki, M.; Tashiro, H.; Suzuki, H. *J. Mol. Catal. B: Enzym.* **1998**, *4*, 181–190.